Hybrid Control of a Pendubot System Using Nonlinear H_∞ and LQR

SEIF-EL-ISLAM HASSENI
Faculty of Sciences and Technology
University of Biskra
P.O. Box 145, Biskra, 07000
ALGERIA

Abstract: - In this paper, a hybrid control approach is synthesized for stabilizing an under-actuated mechanical system, the Pendubot. This kind of system is divided into two modes, the swing-up mode, and the balancing mode. First, dynamic modeling is established by the Euler-Lagrange method. Next, the robust nonlinear H_∞ is designed for the swing-up mode, which handles with the nonlinear model. To weaken the under-actuation characteristic, the control law is developed for the active link with its coupling with the passive link. The LQR is designed for the balancing mode where LQR handles with the linearized model about the unstable top equilibrium position. A simulation is achieved under the MATLAB/Simulink environment. It shows robustness against the external inputs and the fast convergence to the equilibrium position.

Key-Words: - Pendubot; Nonlinear H_∞; LQR; Under-actuated mechanical systems; Robust control; Optimal control.

Received: December 28, 2020. Revised: February 15, 2021. Accepted: February 24, 2021.
Published: March 2, 2021.

1 Introduction

The Under-actuated Mechanical Systems (UMS) have been taken attention by automation and control researchers in the last decades [1, 2]. The under-actuation characteristic means that the mechanical system has control inputs fewer than its degrees of freedom. The taking attention of UMS is due to many reasons such as: decreasing the actuators and subsequently the cost and the weight of the machines/robots or, many of real-life mechanical systems are naturally under-actuated such as mobile robots, walking robots, under-waters, aircrafts and spacecrafts [3]. Besides, the flexibility of the bodies may be considered to augment the compliance in the robot-environment interactions applications. On the other hand, the control of UMS poses difficulties, where the classical approaches, i.e. feedback linearization, are no longer valid or guaranteed the stability of such type of systems, which made the control of these systems complicated and therefore challenging.

The Pendubot system is one of the under-actuated systems which is a two-link planar robot with a single motor at the active link (link 1) and no actuator in the second one, a passive link. This last (link 2) cannot be directly controlled, so, it has a free-move around link 1. The Pendubot has been considered as a simple benchmark for many more complicated robots such as space robots and walking robots [4]. The main control task of the Pendubot system is about the swing-up problem of both links to the neighborhood of the unstable equilibrium top position and then stabilizes the Pendubot system at this equilibrium position [5]. The authors of [6] used the nonlinear approach, sliding mode control, to stabilize the Pendubot system. In [7] the authors analyzed the controllability property for the under-actuated system as a class of the Takagi-Sugeno fuzzy model, where the advantage of the proposed approach is that the convergence can be imposed arbitrarily. In the under-actuated systems, the application of swing-up is more logical. It isn't mentioned in [6, 7] but in [8] the authors proposed a robust swing-up control of the Pendubot system where a nonlinear disturbance observer is used to compensate the effects of the uncertainties. The paper [9] has advantages compared with the other references by exploiting the Pendubot system dynamic to control a planar four-link manipulator and using the modern computing tools (artificial neural networks and fuzzy logic). In this work, after the system is reduced to a virtual Pendubot by using neural networks, a fuzzy logic controller was used to indirectly control the passive links and then the position mode of the servo controller was adopted to control the active links. Contrary to the nonlinear and artificial intelligence tools, in [10], the authors

proposed the stabilization of two under-actuated robots, Furuta pendulum, and Pendubot, by designing a linear state feedback controller. This controller allows eliminating the limit cycle due to the effect of nonlinearity and dead-zone. The authors of [11] designed a controller for the swing-up mode of the Pendubot system by using a new method based on a series rest-to-rest maneuver of the active link about its upright position. To obtain an optimal control, the paper [12] proposed an advanced tracking control of the uncertain nonlinear Pendubot system using a fuzzy LQR control to stabilize it in the top equilibrium position, on the other hand, the sliding mode control optimized by the Differential Evolution algorithm (DE) was used in the balancing mode. Besides, in [13], the authors presented the modeling and simulation for optimal control design of nonlinear inverted pendulum dynamic system using PID and LQR controllers for the stabilization of the Pendubot with a presented disturbance input. In the paper [14], the authors proposed an adaptive fuzzy backstepping controller to control the Pendubot system, where the robustness against the disturbances and uncertainties has been guaranteed. The energy-based controller incorporated with fuzzy neural networks was shown in [15]. The simulations and experimental results of the Pendubot were given to test this controller.

In our paper, a robust controller is designed for the Pendubot system against the external inputs. An optimal LQR is designed for the stabilizing and balancing of the Pendubot. On the other hand, a robust controller based on nonlinear H_∞ theory is used for the swing-up to the top unstable equilibrium position.

The outline of the rest of the paper is as follows; in section 2, the description and the modeling of the Pendubot are presented. In section 3, the controller design is shown in detail. The simulation tests are applied and the results showing in section 4. Finally, a conclusion is given in section 5.

2 Modeling of the Pendubot system

The Pendubot is a planar manipulator with two links, an active link, and a passive link. It has only one rotational actuator in the active joint. Therefore, it has been considered a typical under-actuated benchmark for control and robotic researchers. The Pendubot structure is shown in Fig. 1, where:

m_1: the mass of link 1.
m_2: the mass of link 2.
l_1: length of link 1.
l_2: length of link 2.
l_{c1}: distance to the mass' center of link 1.
l_{c2}: distance to the mass' center of link 2.
I_1: the moment of inertia of link 1.
I_2: the moment of inertia of link 2.
g: gravity constant.
q_1: the angle of the active link, link 1.
q_2: the angle of the passive link makes with link 1.
τ_1: the applied torque on the active joint.

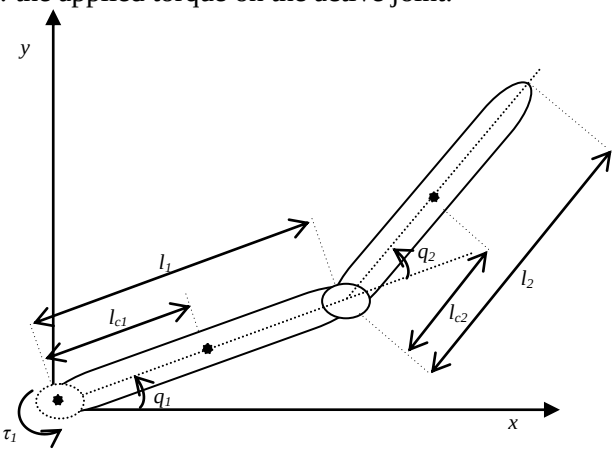

Fig. 1 Geometric scheme of the Pendubot

2.1 The motion equations

The Pendubot model is obtained by Euler-Lagrange formulation:

$$L = E_k - E_p \tag{1}$$

E_k is the kinetic energy, and E_p is the potential energy, where:

$$\begin{aligned} E_k = \frac{1}{2}(&I_1 + m_1 l_{c1}^2 + m_2 l_1^2 + I_2 + m_2 l_{c2}^2 \\ &+ 2m_2 l_1 l_{c2} cos q_2)\dot{q}_1^2 \\ &+ (I_2 + m_2 l_{c2}^2 + m_2 l_1 l_{c2} cos q_2)\dot{q}_1 \dot{q}_2 \\ &+ (I_2 + m_2 l_{c2}^2)\dot{q}_2^2 \end{aligned} \tag{2}$$

$$E_p = (m_1 l_{c1} + m_2 l_1) g \, sin \, q_1 + m_2 l_{c2} g \sin(q_1 + q_2) \tag{3}$$

The equations are obtained from the Lagrangian equation:

$$\frac{d}{dt}\left(\frac{\partial L}{\partial \dot{q}}\right) - \frac{\partial L}{\partial q} = \tau \tag{4}$$

Where, $q = [q_1 \quad q_2]^T$ the vector of the angles coordinates $\dot{q} = [\dot{q}_1 \quad \dot{q}_2]^T$ is the vector of their derivatives and $\tau = [\tau_1 \quad 0]^T$ is the vector of the non-conservatives torques, where there is just one torque.

The dynamic equations of the Pendubot are presented as follows:

$$M(q)\ddot{q} + C(q,\dot{q})\dot{q} + G(q) = \begin{bmatrix} \tau_1 \\ 0 \end{bmatrix} \tag{5}$$

Where:

$$M(q) = \begin{bmatrix} M_{11} & M_{12} \\ M_{21} & M_{22} \end{bmatrix} = \begin{bmatrix} a_1 + a_2 + 2a_3 \cos q_2 & a_2 + a_3 \cos q_2 \\ a_2 + a_3 \cos q_2 & a_2 \end{bmatrix} \quad (6)$$

$$C(q, \dot{q})\dot{q} = \begin{bmatrix} C_{11} & C_{12} \\ C_{21} & C_{22} \end{bmatrix} = \begin{bmatrix} -a_3 \sin(q_2)\dot{q}_2 & -a_3 \sin(q_2)\dot{q}_2 - a_3 \sin(q_2)\dot{q}_1 \\ a_3 \sin(q_2)\dot{q}_1 & 0 \end{bmatrix} \quad (7)$$

$$G(q) = \begin{bmatrix} G_1 \\ G_2 \end{bmatrix} = \begin{bmatrix} a_4 g cos\, q_1 + a_5 g cos(q_1 + q_2) \\ a_5 g cos(q_1 + q_2) \end{bmatrix} \quad (8)$$

And, $a_1 = I_1 + m_1 l_{c1}^2 + m_2 l_1^2$, $a_2 = I_2 + m_2 l_{c2}^2$, $a_3 = m_2 l_1 l_{c2}$, $a_4 = m_1 l_{c1} + m_2 l_1$, $a_5 = m_2 l_{c2}$.

The parameters are considered from an experimental project of Illinois university [16]: a_1=0.034, a_2=0.0125, a_3=0.01, a_4=0.215, a_5=0.073 and g=9.8.

2.2 The linearized model

The Pendubot system has four equilibrium positions; a stable equilibrium position, $[q_1, \dot{q}_1, q_2, \dot{q}_2] = \left[\frac{-\pi}{2}, 0, 0, 0\right]$, an unstable position, $[q_1, \dot{q}_1, q_2, \dot{q}_2] = \left[\frac{\pi}{2}, 0, \pi, 0\right]$, an unstable mid position, $[q_1, \dot{q}_1, q_2, \dot{q}_2] = \left[\frac{-\pi}{2}, 0, \pi, 0\right]$, and an unstable top position, $[q_1, \dot{q}_1, q_2, \dot{q}_2] = \left[\frac{\pi}{2}, 0, 0, 0\right]$. We wish to avoid the three first equilibrium positions and focus on just the top equilibrium position, where the objective is to stabilize the Pendubot on it.
First, we rewrite (5) as follows:

$$\ddot{q}_1 = \frac{1}{a_1 a_2 - a_3^2 cos^2 q_2}[a_2 a_3 sin q_2 (\dot{q}_1 + \dot{q}_2)^2 + a_3^2 cos q_2 \sin(q_2)\, \dot{q}_1^2 - a_2 a_4 g\, cos q_1 + a_3 a_5\, g\, cos q_2 \cos(q_1 + q_2) + a_2 \tau_1] \quad (8)$$

$$\ddot{q}_2 = \frac{1}{a_1 a_2 - a_3^2 cos^2 q_2}[-a_3 (a_2 + a_3 cos q_2) sin q_2 (\dot{q}_1 + \dot{q}_2)^2 - (a_1 + a_3 cos q_2) a_3 \sin(q_2)\, \dot{q}_1^2 + (a_2 + a_3 cos q_2)(a_4\, g\, cos q_1 - \tau_1) - (a_1 + a_3 cos q_2) a_5 g \cos(q_1 + q_2)] \quad (9)$$

We are linearizing the nonlinear differential equations (8)-(9) about the top equilibrium position. With the applied parameters, the obtained linear system is as follows:

$$\begin{bmatrix} \dot{q}_1 \\ \ddot{q}_1 \\ \dot{q}_2 \\ \ddot{q}_2 \end{bmatrix} = \begin{bmatrix} 0 & 1 & 0 & 0 \\ -13.74 & 0 & -22.01 & 0 \\ 0 & 0 & 0 & 1 \\ -49.01 & 0 & 96.85 & 0 \end{bmatrix} \begin{bmatrix} q_1 \\ \dot{q}_1 \\ q_2 \\ \dot{q}_2 \end{bmatrix} + \begin{bmatrix} 0 \\ 38.46 \\ 0 \\ -69.23 \end{bmatrix} \tau_1 \quad (10)$$

3 The control algorithms of the Pendubot

In this section, the different control approaches used are presented. The nonlinear H_∞ control is used for the swing-up mode. When the Pendubot is near the top equilibrium position LQR is used to balancing and stabilizing the Pendubot at this equilibrium position.

3.1 Nonlinear H_∞ control for the swing-up mode

Because the Pendubot is an under-actuated robot manipulator the nonlinear H_∞ controller is designed for the controlled degrees of freedom, the angle q_1, with its coupling with the passive degree of freedom, the angle q_2.

By extracting the dynamic of the active degree of freedom from (5), the first row, we have

$$\tau_1 + \delta = M_{11}(q)\ddot{q}_1 + M_{12}(q)\ddot{q}_2 + C_{11}(q, \dot{q})\dot{q}_1 + C_{12}(q, \dot{q})\dot{q}_2 + G_1(q) \quad (10)$$

We add here the extern input signal (δ). The acceleration of q1 can be extracted from (10):

$$\ddot{q}_1 = -M_{11}^{-1}(q)(C_{11}(q, \dot{q})\dot{q}_1 + G_1(q) - \tau_1 - \delta + M_{12}(q)\ddot{q}_2 + C_{12}(q, \dot{q})\dot{q}_2) \quad (11)$$

The errors are considered as the states of the system as follows, where we included the integral:

$$x = \begin{bmatrix} \dot{\tilde{q}}_1 \\ \tilde{q}_1 \\ \int \tilde{q}_1 dt \end{bmatrix} = \begin{bmatrix} \dot{q}_1 - \dot{q}_1^d \\ q_1 - q_1^d \\ \int (q_1 - q_1^d) dt \end{bmatrix} \quad (12)$$

where q_1^d and $\dot{q}_1^d$ are the corresponding desired trajectory and velocity respectively. We included the integral term to allow the obtaining a null steady-state error when the disturbances act [17].
A state transformation is made before the designing of the control laws:

$$z = T_0 x = \begin{bmatrix} T_1 & T_2 & T_3 \\ 0 & 1 & 1 \\ 0 & 0 & 1 \end{bmatrix} \begin{bmatrix} \dot{\tilde{q}}_1 \\ \tilde{q}_1 \\ \int \tilde{q}_1 dt \end{bmatrix} \quad (13)$$

The state-space representation can be written as follows:

$$\dot{x} = f(x) + g(x) T_1 \left(\tau_1 - F(x_e)\right) + k(x) w \quad (14)$$

where:

$$F(x_e) = M_{11}(q)\left(\ddot{q}_1^d - T_1^{-1}T_2\dot{\tilde{q}}_1 - T_1^{-1}T_3\tilde{q}_1\right) + C_{11}(q,\dot{q})\left(\dot{q}_1^d - T_1^{-1}T_2\tilde{q}_1 - T_1^{-1}T_3\int\tilde{q}_1 dt\right) + G_1(q) + M_{12}(q)\ddot{q}_2 + C_{12}(q,\dot{q})\dot{q}_2 \quad (15)$$

with $x_e = (\tilde{q}_1, \dot{\tilde{q}}_1, \int\tilde{q}_1 dt\,, \dot{q}_1^d, \ddot{q}_1^d)$.

And:

$$f(x) = T_0^{-1}\begin{bmatrix} -M_{11}^{-1}(q)C_{11}(q,\dot{q}) & 0 & 0 \\ T_1^{-1} & 1 - T_1^{-1}T_2 & T_1^{-1}(T_2 - T_3) - 1 \\ 0 & 1 & -1 \end{bmatrix} T_0 x$$

$$g(x) = k(x) = T_0^{-1}\begin{bmatrix} M_{11}^{-1}(q) \\ 0 \\ 0 \end{bmatrix}$$

Where $w = T_1\delta$: external inputs. The control law is considered as:

$$u = T_1(\tau_1 - F(x_e)) \quad (16)$$

The state-space representation can be written as follows:

$$\dot{x} = f(x) + g(x)u + k(x)w \quad (17)$$

Eq. (17) presents the dynamic representation of the H_∞ problem. We can now apply the theoretical results of the nonlinear H_∞ control presented in [18]. After computing T by solving Hamilton-Jacobi-Bellman-Isaacs (HJBI) equations [17], the optimal control law u^* is as follows:

$$u^* = -R^{-1}(S^T + T)x \quad (18)$$

We replace (18) in (16) and we apply the expression of τ_1 in (11), we have:

$$M_{11}(q)T\dot{x} + C_{11}(q,\dot{q})Tx = u + w \quad (19)$$

where $w = T_1\delta$. To compute the torque τ_1, we are extracting the acceleration control $\ddot{q}_1$:

$$\ddot{q}_1 = \ddot{q}_1^d - K_D\dot{\tilde{q}}_1 - K_P\tilde{q}_1 - K_I\int\tilde{q}_1 dt \quad (20)$$

with:

$$K_D = T_1^{-1}(T_2 + M_{11}^{-1}(q)C_{11}(q,\dot{q})T_1 + M_{11}^{-1}(q)R^{-1}(S_1 + T_1))$$
$$K_P = T_1^{-1}(T_3 + M_{11}^{-1}(q)C_{11}(q,\dot{q})T_2 + M_{11}^{-1}(q)R^{-1}(S_2 + T_2))$$
$$K_I = T_1^{-1}\left(M_{11}^{-1}(q)C_{11}(q,\dot{q})T_3 + M_{11}^{-1}(q)R^{-1}(S_3 + T_3)\right) \quad (21)$$

We choose the weighting matrix W^TW as follows:

$$Q = \begin{bmatrix} \omega_1^2 & 0 & 0 \\ 0 & \omega_2^2 & 0 \\ 0 & 0 & \omega_3^2 \end{bmatrix}, S = \begin{bmatrix} 0 \\ 0 \\ 0 \end{bmatrix}, R = \omega_u^2 \quad (22)$$

The solutions of the HJBI equations, according to [17] are:

$$\begin{cases} T_1 = \sqrt{Q_1} = \omega_1 \\ T_2 = \sqrt{\omega_2^2 + 2\omega_1\omega_3} \\ T_3 = \sqrt{Q_3} = \omega_3 \end{cases} \quad (23)$$

The gains are:

$$K_D = \frac{\sqrt{\omega_2^2+2\omega_1\omega_3}}{\omega_1} + M_{11}^{-1}(q)\left(C_{11}(q,\dot{q}) + \frac{1}{\omega_u^2}\right)$$
$$K_P = \frac{\omega_3}{\omega_1} + \frac{\sqrt{\omega_2^2+2\omega_1\omega_3}}{\omega_1}M_{11}^{-1}(q)\left(C_{11}(q,\dot{q}) + \frac{1}{\omega_u^2}\right)$$
$$K_I = \frac{\omega_3}{\omega_1}M_{11}^{-1}(q)\left(C_{11}(q,\dot{q}) + \frac{1}{\omega_u^2}\right) \quad (24)$$

After getting the expression of $\ddot{q}_1$, the expression of the applied torque τ_1 to the Pendubot is as follows:

$$\tau_1 = M_{11}(q)\ddot{q}_1 + C_{11}(q,q)\dot{q}_1 + G_1(q) + M_{12}(q)\ddot{q}_2 + C_{12}(q,\dot{q})\dot{q}_2 \quad (25)$$

The weighting parameters of the nonlinear H_∞ controller: ω_1=0.1, ω_2=2, ω_3=9, ω_u=1.5.

3.2 LQR for the balancing mode

The LQR controller handles with the linearized model (10), about the top equilibrium position. It aims to find an optimal controller to minimize the cost function J:

$$J = \frac{1}{2}\int_0^\infty (xQx + u^TRu)dt \quad (26)$$

Where x presents here the errors vector between the actual and desired signals, the top position:

$$x = \begin{bmatrix} q_1 \\ \dot{q}_1 \\ q_2 \\ \dot{q}_2 \end{bmatrix} - \begin{bmatrix} \frac{\pi}{2} \\ 0 \\ 0 \\ 0 \end{bmatrix} \quad (27)$$

The Q and R are positive definite matrices. To design the LQR controller, we should solve the Riccati equation [19]:

$$-PA - A^TP - Q + PBR^{-1}B^TP = 0 \quad (28)$$

According to it, the optimal control law (u^*=τ_1) is defined as follows:

$$u^* = -Kx \quad (29)$$

Where:

$$K = R^{-1}B^T P \quad (30)$$

We choose the weightings, Q and R as follows:

$$Q = \begin{bmatrix} 1 & 0 & 0 & 0 \\ 0 & 0 & 0 & 0 \\ 0 & 0 & 1 & 0 \\ 0 & 0 & 0 & 0 \end{bmatrix}, \; R = 1 \quad (31)$$

According to it, the controller K is as follows:

$$K = [16.4 \quad 3.13 \quad 16.2 \quad 2.07] \quad (32)$$

As mentioned before, the nonlinear H_∞ controller is designed for the swing-up mode, and LQR is used for the balancing mode. Fig. 2 presents control architecture.

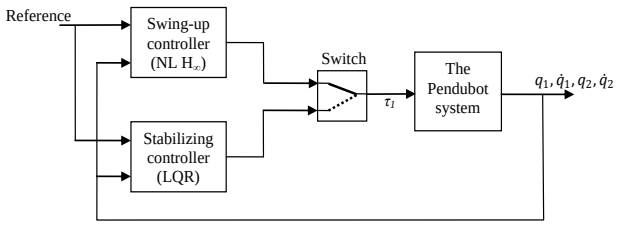

Fig. 2 The control architecture of the Pendubot

4 Simulation results

To test the proposed controllers, a simulation has been performed under the MATLAB/Simulink environment. The considered initial position of the Pendubot, $[q_1^0, \dot{q}_1^0, q_2^0, \dot{q}_2^0] = \left[-\frac{\pi}{2}, 0, 0, 0\right]$, is the passive stable equilibrium position. The desired position is the unstable top position, $\left[q_1^d, \dot{q}_1^d, q_2^d, \dot{q}_2^d\right] = \left[\frac{\pi}{2}, 0, 0, 0\right]$. To test the robustness against the external inputs, we applied a permanent disturbance in the input. Noises are applied in q_1 in the instance *8s* and q_2 in the instance *5s*.

First, the H_∞ controller works and brings the Pendubot near to the top position, but the second link still swings. An instance when the Pendubot is close enough to the top position, $|q_2| < 0.2$, switching to the linear controller (LQR). In this simulation the chosen instance is *4.57s*.

Fig. 3 presents the angle and the velocity dynamics of the first link where it shows how the angle converges to $\frac{\pi}{2}$, and its velocity converges to 0 quickly. Fig. 4 presents the angle and the velocity dynamics of the second link. The link swings first and then in the instance 4.57s when the LQR switched, the link converges and stabilizes in the null angle. There are some variations in the dynamics due to the noises and the disturbance but thanks to the robust controller, nonlinear H_∞, the external inputs are rejected with robustness. To show the precision more, Fig. 5 presents the error signals of both q_1 and q_2. Fig. 6 presents the applied torque, it is going to zero when the Pendubot stabilizes.

The objective of the swing-up mode is to make the second link (passive) tracks a very specific trajectory, a homoclinic orbit, which means that the angle of link 2 moves clockwise or counter-clockwise till it reaches the equilibrium position which is zero in both angular position and velocity. Fig. 7 shows that the applied nonlinear controller (nonlinear H_∞) can bring the Pendubot system to orbit.

Compared with experimental results in [16], the proposed controller provided a dynamic behavior near to the experimental results. In Fig.3, Settling time of q_1 ($ST_{q1} = 0.2s$), overshoot ($OV_{q1} = 27\%$), in Fig.4, the period of oscillation of q_2 ($t_{q2} = 2s$). In [16], ($ST_{q1} = 2s$, $OV_{q1} = 2\%$, $t_{q2} = 2s$).

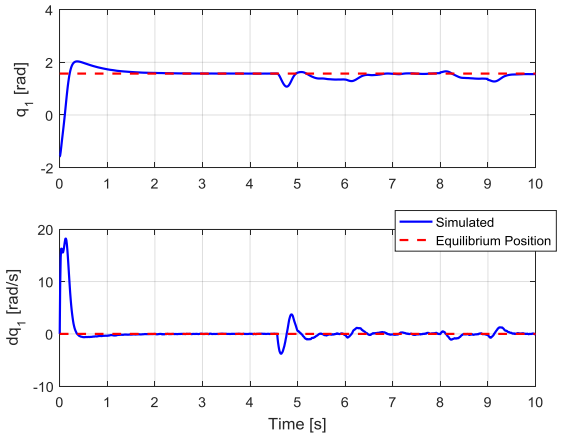

Fig. 3 The angular position and velocity of link 1

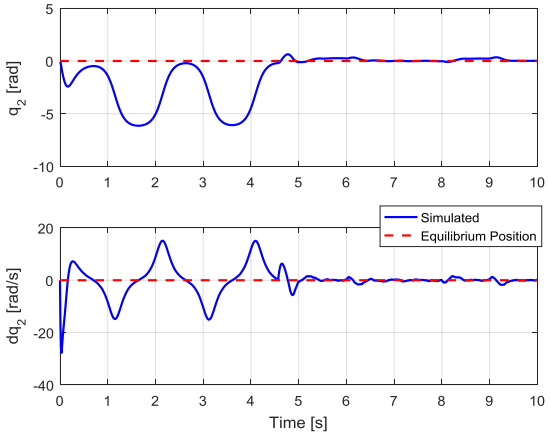

Fig. 4 The angular position and velocity of link 2

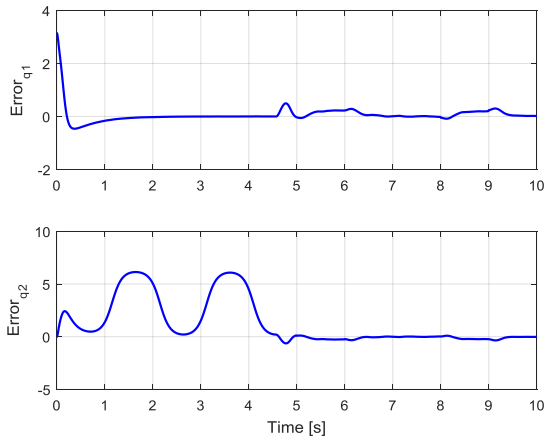

Fig. 5 The error signals of q_1 and q_2

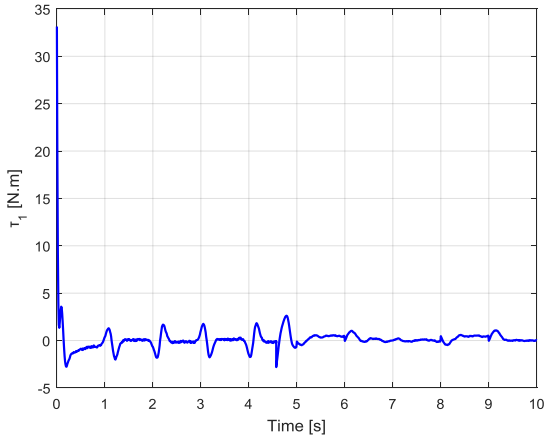

Fig. 6 The applied torque τ_1

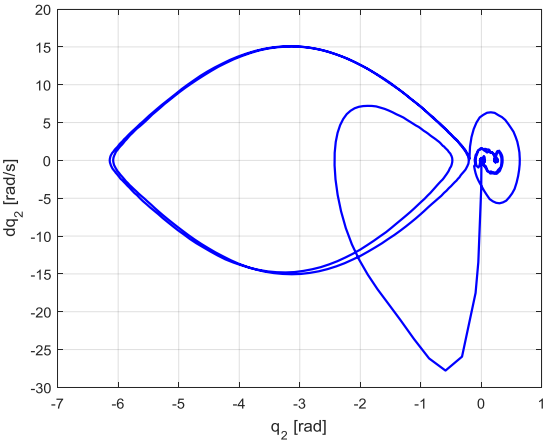

Fig. 7 The phase plot (homoclinic orbit)

5 Conclusion

In this paper, the control of such an under-actuated mechanical system is achieved. The control is done with two approaches, nonlinear H_∞ and LQR. The first one, H_∞, is used for the swing-up mode and to make the Pendubot close to the balancing mode, where LQR is used to stabilize the Pendubot in the top equilibrium position. The simulation results show that the proposed controllers are robust against the disturbance and noises thanks to the potential of nonlinear H_∞ to weaken the external inputs, which are rejected and the Pendubot converges to its equilibrium position in a short period.

References:

[1] Xin X, and Liu Y, *Control Design and Analysis for Underactuated Robotic Systems*, Springer, 2014.

[2] Seifried R, *Dynamics of Underactuated Multibody Systems, Modeling, Control and Optimal Design*, Springer, 2014.

[3] Duan C, Hu Q, Zhang Y, and Wu H, "Constrained single-axis path planning of underactuated spacecraft," *Aerospace Science and Technology*, Vol. 107, 2020.

[4] Kant N, Mukherjee R, Chowdhury D, and Khalil HK, "Estimation of the Region of Attraction of Underactuated Systems and Its Enlargement Using Impulsive Inputs," *IEEE Transactions on Robotics*, Vol. 35, No. 3, 2019, pp. 618-632.

[5] Spong MW, and Block DJ, "The pendubot: a mechatronic system for control research and education," in *Proceedings of IEEE Conference on Decision and Control*, New Orleans, USA, 1995, pp. 555-556.

[6] Yoo DS, "Balancing Control for the Pendubot using Sliding Mode," in *Proceedings of International Symposium on Robotics*, Seoul, South Korea, 2013.

[7] Meda-Campaña JA, Rodríguez-Valdez J, Hernández-Cortés T, Tapia-Herrera R, and Nosov V, "Analysis of the Fuzzy Controllability Property and Stabilization for a Class of T-S Fuzzy Models," *IEEE Transactions on Fuzzy Systems*, Vol. 23, No. 2, 2015, pp. 291-300.

[8] Eom M, and Chwa D, "Robust Swing-Up and Balancing Control Using a Nonlinear Disturbance Observer for the Pendubot System With Dynamic Friction," *IEEE Transactions on Robotics*, Vol. 31, No. 2, 2015, pp. 331-343.

[9] Wu J, She J, Wang Y, and Su CY, "Position and Posture Control of Planar Four-Link Underactuated Manipulator Based on Neural Network Model," *IEEE Transactions on Industrial Electronics*, Vol. 67, No. 6, 2019, pp. 4721-4728.

[10] Antonio-Cruz M, Hernández-Guzmán VM, and Silva-Ortigoza R, "Limit Cycle Elimination in Inverted Pendulums: Furuta Pendulum and Pendubot," *IEEE Access*, Vol. 6, 2018, pp. 30317-30332.

[11] Albahkali T, Mukherjee R, and Das T, "Swing-Up Control of the Pendubot: An Impulse-Mommentum Approach," *IEEE Transactions on Robotics*, Vol. 25, No. 4, 2009, pp. 975-982.

[12] Nguyen NS, Van-Kien C, and Huy-Anh HP, "Uncertain nonlinear system control using hybrid fuzzy LQR-sliding mode technique optimized with evolutionary algorithm," *Engineering Computations*, Vol. 36, No. 6, 2019, pp. 1893-1912.

[13] Prasad LB, Tyagi B, and Gupta HO, "Optimal Control of Nonlinear Inverted Pendulum System Using PID Controller and LQR: Performance Analysis Without and With Disturbance Input," *International Journal of Automation and Computing*, Vol. 11, No. 6, 2014, pp. 661-670.

[14] Azimi MM, and Koofigar HR, "Adaptive fuzzy backstepping controller design for uncertain underactuated robotic systems," *Nonlinear Dynamics*, Vol. 79, No. 2, 2015, pp. 1457-1468.

[15] Xia D, Chai T, and Wang L, "Fuzzy Neural-Network Friction Compensation-Based Singularity Avoidance Energy Swing-Up to Nonequilibrium Unstable Position Control of Pendubot," *IEEE Transactions on Control Systems Technology*, Vol. 22, No. 2, 2014, pp. 690-705.

[16] Fantoni I, and Lozano R, "The pendubot system," in Fantoni I, and Lozano R (eds.), *Non-linear Control for Underactuated Mechanical Systems*, Springer, 2002, pp. 53-72.

[17] Ortega MG, Vargas M, Vivas C, and Rubio FR, "Robustness improvement of a nonlinear H_∞ controller for robot manipulators via saturation functions," *Journal of Robotic Systems*, Vol. 22, No. 8, 2005, pp. 421-437.

[18] van der Schaft AJ, *L_2 gain and passivity techniques in nonlinear control*, Springer, 2000.

[19] Lavretsky E, and Wise KA, "Optimal Control and the Linear Quadratic Regulator," in Lavretsky E, and Wise KA (eds.), *Robust and Adaptive Control With Aerospace Applications*, Springer, 2013, pp. 27-50.